

# We are IntechOpen, the world's leading publisher of Open Access books Built by scientists, for scientists

**4,800**

Open access books available

**122,000**

International authors and editors

**135M**

Downloads

Our authors are among the

**154**

Countries delivered to

**TOP 1%**

most cited scientists

**12.2%**

Contributors from top 500 universities



**WEB OF SCIENCE™**

Selection of our books indexed in the Book Citation Index  
in Web of Science™ Core Collection (BKCI)

Interested in publishing with us?  
Contact [book.department@intechopen.com](mailto:book.department@intechopen.com)

Numbers displayed above are based on latest data collected.

For more information visit [www.intechopen.com](http://www.intechopen.com)



---

# Carbon Nanotube Transparent Electrode

---

Jing Sun and Ranran Wang

Additional information is available at the end of the chapter

<http://dx.doi.org/10.5772/51783>

---

## 1. Introduction

In the modern world, transparent conductive films (TCF) are extremely common and critically important in electrical devices. In our homes or offices, they are found in flat panel displays such as in TVs, laptops and in touch panels, of phones, tablet computers, E-readers and digital cameras [1]. Besides, they are also used as the electrodes for photovoltaic devices such as solar cells [2] and organic light-emitting diodes (OLEDs) [3]. Liquid crystal display (LCD) is by far the largest user of transparent conductive films but many devices are showing rapid growth in popularity such as touch panels (362 million units in 2010 with annual growth of 20% through 2013), E-paper (30 fold growth expected from 2008 to 2014), and thin film solar cells (expected sales of over \$13 billion by 2017) [4].

The dominant transparent conductive material used today is tin doped indium oxide (ITO) with a demand growing at 20% per annum [5]. ITO has been studied and refined for over 70 years, and as a result, the material offers many beneficial properties. However, ITO has certain drawbacks, mainly reflected on the depleted supply of raw material and their brittleness. The supply of indium is constrained by both mining and geo-political issues, which leads to dramatic price fluctuations over the last decades, from \$ 100- \$ 900, as shown in Figure 1. The high price of indium determined the high cost of ITO, since they compose nearly 75wt % of a typical ITO film [6]. In addition to the raw materials, the expense of setting up and maintaining a sputtering deposition line, as well as the low deposition yield (3-30%) [7] also increases the cost of ITO. Though current devices are typically based on rigid substrates, there is a continued trend toward flexible devices. As ITO tend to fracture at strains of 2%, they are completely unsuitable for using in flexible electronics. Therefore, new transparent electrode materials have rapidly emerged in recent years, including carbon nanotubes (CNTs), graphene and metal nanowires. The intrinsically high conductivity cou-

pled with high aspect ratio yields films with high transmittance, adequately low sheet resistance, and superior mechanical flexibility. These material properties, combined with inexpensive material and deposition costs make these emerging nanomaterials very attractive for as transparent electrodes. Of the three dominant nanoscale materials, CNTs are perhaps the most promising and mature intensively investigated.

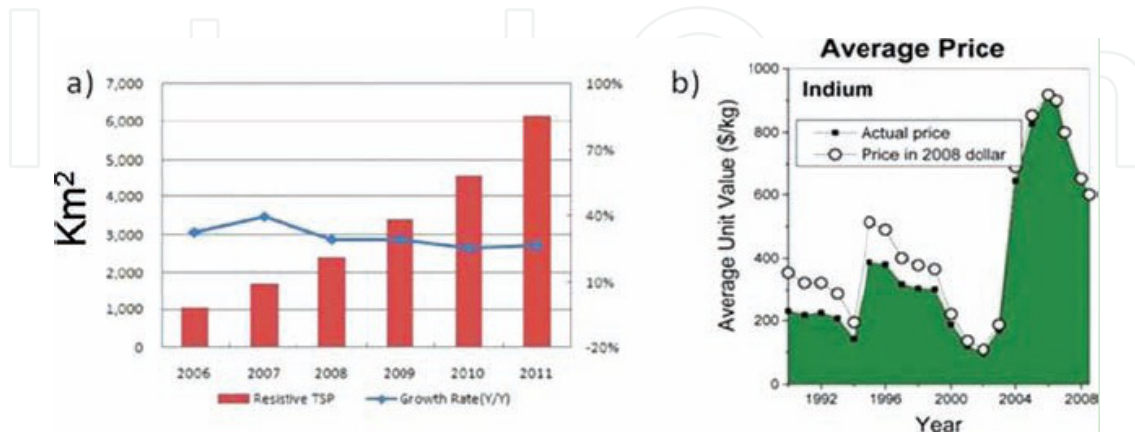


**Figure 1.** (a) Global demand for resistive style touch panels by area; (b) Average price of Indium over the last several decades; Reprinted with permission from reference [4] copyright 2011 Wiley.

This review will focus on transparent electrode made of CNTs, and six main parts will be covered.

1. At first, some basic theories and parameters for characterizing transparent conductive materials will be presented so that the following parts of the review can be profoundly understood.
2. CNTs prepared from different methods or modified under various conditions have diverse physical and chemical properties, which will yield films with distinct performance. Therefore, in the second part, CNTs of different types will be investigated, and the performance of the as prepared thin films will be compared.
3. One of the major advantages in using CNTs is their ability to be applied to substrates from solution, which opens up many alternative deposition techniques. Therefore, one of the primary research areas for making transparent conductive films is to process the CNT material into printable inks. The third part will outline major approaches to disperse CNTs and focus on the most important details with regards to making transparent conductive films.
4. In the fourth part, a variety of techniques for making transparent conductive CNT films will be presented and evaluated.
5. During the solubilization step, non-conducting dispersants are induced, which sacrifice the conductance of the films a lot. Therefore, post-treatment needs to be done to remove them for enhancing the performance of the films. In the fifth part, various methods used to improve the performance of the transparent conductive films after their preparation will be discussed.

Finally, the latest progress on CNT transparent conductive films and their applications on electrical devices will be summarized.

## 2. Optoelectronic properties

The two most important features for a transparent conducting material are its sheet resistance ( $R_s$ ) and optical transparency. The sheet resistance is defined as  $R_s = R(W/L)$ , where  $R$  is DC resistance,  $W$  and  $L$  are width and length of the film. Grüner et al. [8] developed a suitable merit, the DC conductivity/optical conductivity ( $\sigma_{dc}/\sigma_{op}$ ), to compare the performance of various transparent conductors based on the standard percolation theory, in which each bundle of nanotubes was counted as one conducting stick. They assumed the conductivity ratio  $\sigma_{dc}/\sigma_{op}$  remains constant for nanotube networks with different densities in the measured optical frequency range. By plotting  $R_s$  vs  $T$  and fitting the data to equation 1, one can estimate the value of  $\sigma_{dc}/\sigma_{op}$ . This value is often used as a Figure of Merit for transparent conductors since high values of  $\sigma_{dc}/\sigma_{op}$  leads to films with high  $T$  and low  $R_s$ .

$$T = \frac{1}{1 + \frac{2\pi\sigma_{op}}{cR_s\sigma_{dc}}} \quad (1)$$

Geng et al. [9] found that this equation can be fitted well to the curve of single-walled carbon nanotube TCFs, nevertheless can not be fitted well with carbon nanotubes of other types. They modified the equation as follows:

$$T = t \cdot \left(1 + \frac{188 (\Omega) \sigma_{op}}{R_s \sigma_{dc}}\right)^{-2} \quad (2)$$

The parameter  $t$  may represent the optical property of CNT films. A high  $t$  value gives a high transmittance for the CNT films. The  $t$  value of SWCNT films is 0.999, while that of MWCNT is much lower, around 0.884.

Recently, Coleman et al. [5] modified this model to evaluate thinner (more transparent) films. They found that the data tend to deviate severely from the fits for thinner films, as seen from Figure 2. This deviation has been observed before [10-12] and tends to occur for films with  $T$  between 50% and 92%. Thus,  $\sigma_{dc}/\sigma_{ac}$  fails to describe the relationship between  $T$  and  $R_s$  in the relevant regime. The deviation from bulk-like behavior as described in Equation 1, can be explained by percolation effects [13]. Such effects become important for very sparse networks of nano conductors. When the number of nanoconductors per unit is very low, a continuous conducting path from one side of the sample to the other will generally not exist.

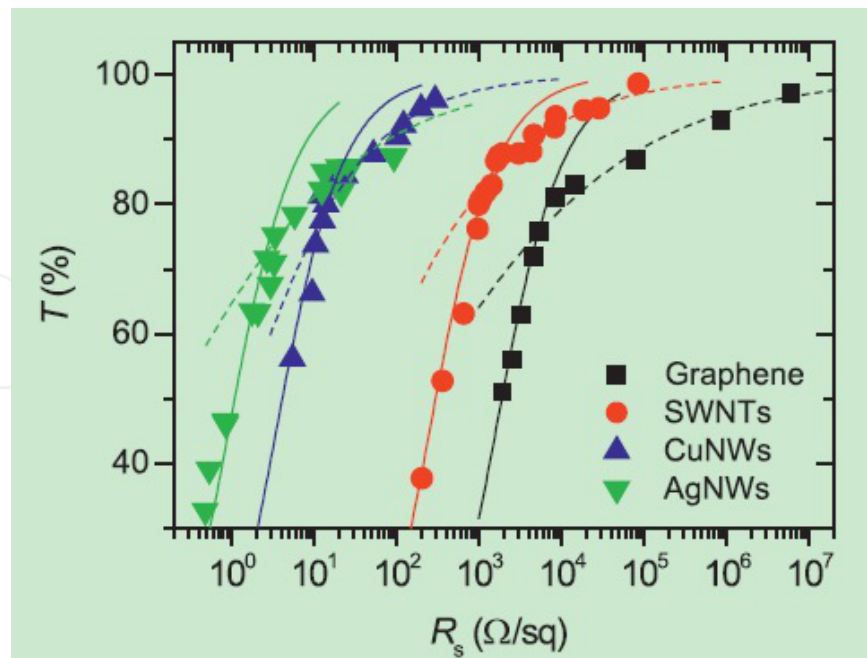


**Figure 2.** Typical graph of transmittance (generally measured at 550 nm) plotted versus sheet resistance for thin films of nanostructured materials. Reprinted with permission from reference [5] copyright MRS.

As more nanoconductors are added, at some point (the percolation threshold) the first conducting path will be formed. As more material is added, more conductive paths are formed, and the conductivity of the network increases rapidly. Eventually it reached a “bulk-like” value above which it remains constant. Percolation theory describes how the dc conductivity of sparse networks depends on network thickness and predicts a non-linear, power law dependence:

$$\sigma_{dc} \propto (t - t_c)^n \quad (3)$$

where  $t$  is the estimated thickness of the network,  $t_c$  is the thickness associated with the percolation threshold, and  $n$  is the percolation exponent. This leads to a new relationship between  $T$  and  $R_s$ , which applies to thin, transparent networks:

$$T = \left[ 1 + \frac{1}{\Pi} \left( \frac{Z_0}{R_s} \right)^{1/(n+1)} \right]^{-2} \quad (4)$$

where  $\Pi$  is the percolative FoM:

$$\Pi = 2 \left[ \frac{\sigma_{dc} / \sigma_{op}}{(Z_0 t_{min} \sigma_{op})^n} \right]^{1/(n+1)} \quad (5)$$

Here,  $t_{min}$  is the thickness below which the dc conductivity becomes thickness dependent. It scales closely with the nanostructures' smallest dimension,  $t_{min} \approx 2.33 D$ . The high  $T$  portion

of data in Figure 1 was fitted using Equation 4, and good fits allow the calculation of both  $n$  and  $\Pi$ . Analysis of these equations shows that large values of  $\Pi$  but low values of  $n$  are desirable to achieve low  $R_s$  coupled with high  $T$ , which are used to evaluate the performance of CNT films with high performance.

In addition to their sheet resistance and optical transparency, the stability and mechanical durability are also critical criteria to evaluate the performance of transparent conductors. Undoped CNT films exhibit excellent stability upon exposure to atmospheric conditions, as seen in Figure 3 [14]. Doping with nitric acid or  $\text{SOCl}_2$  could decrease the sheet resistance significantly, however at the expense of sacrificing their stability [15-17]. The sheet resistance of undoped SWCNT films decreases slightly with increasing temperature, which is consistent with the electrical behavior of semiconductors. Thermal stability of doped CNTs is dependent on dopants since elevated temperatures may increase chemical reactions or enhance the desorption of dopants out of the films. CNT-PET thin films are significantly more flexible than commercial ITO/PET films. They can be bent all the way to  $180^\circ$  without a significant change in resistance, [18] and the conductivity of the films can be retained after 500 bending cycles [19].

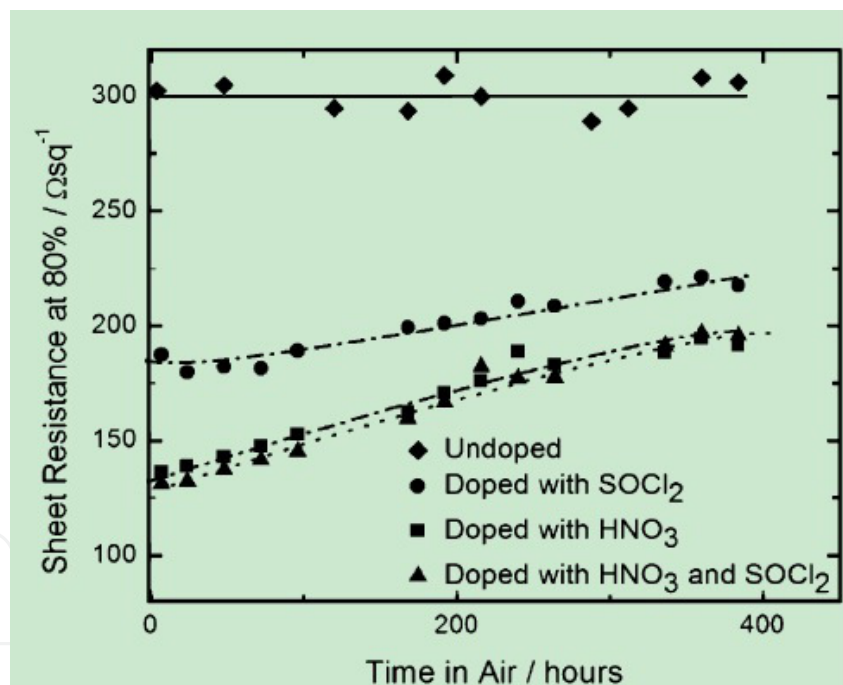


**Figure 3.** Absolute sheet resistance versus time in air of four SWNT films. Reprinted with permission from reference [14] copyright Wiley.

### 3. The choice of Carbon Nanotubes

Carbon nanotubes synthesized from different methods or processes have diverse material qualities, such as the degree of purity, the defects, their length and diameters, and the chiral-

ities, which are presumably important factors in determining the film performance. Therefore, the choice of CNTs as well as their further treatment is markedly important. Young Hee Lee group [9,20] did systematical analysis to investigate the CNT quality dependence. In their work, single-walled carbon nanotubes (SWCNT), double-walled carbon nanotubes (DWCNT), thin multiwalled carbon nanotubes (t-MWCNT) and multiwalled carbon nanotubes (MWCNT) powders were separately dispersed in deionized water with sodium dodecyl sulfate (SDS) and dichloroethane (DCE) by sonication and sprayed onto poly (ethylene terephthalate) (PET) substrates to fabricate thin films. The sheet resistance and transmittance of each film was measured and compared. As seen in Figure 4, the film's performance changes dramatically for different types of CNTs dispersed in deionized water with SDS, as well as in DCE. The TCFs fabricated with SWCNTs show the best film performance among all the selected CNTs. The trends of film performances are similar for the TCFs fabricated by using the CNT solution dispersed in deionized water and in DCE, which is  $\text{SWCNTTCF} > \text{DWCNTTCF} > \text{t-MWCNTTCF} > \text{MWCNTTCF}$ . Furthermore, they analyzed the defects and metallicity by Raman spectra, and found that CNTs with fewer defects and high content of metallic tubes leads to TCFs with higher conductivity. Nevertheless, in Li's report, [21]. MWCNTTCFs exhibit better performance than SWCNTTCFs. They indicated that MWCNT have more conductive  $\pi$  channels than SWCNTs does, therefore MWCNTs have better electronic transportability. In the case of a MWCNT where conduction occurs through the outer most shell, the large diameter of the outernanotube causes the gap to approach 0 eV and the nanotube to become basically metallic. On the contrary, 2/3 of SWCNTs are semi-conducting. The other reason they mentioned is that the MWCNTs they used are longer than SWCNTs, which could decrease the contacts numbers. Another point needs to be addressed is that dimethylformamide (DMF) which was chosen as the solvent in their work is actually not efficient to exfoliate SWCNTs. Therefore, SWCNTs bundled together which would open up an energy gap or pseudo gap owing to intertube interactions. We believe this is a critical reason for the worse performance of SWCNTTCFs in their work.

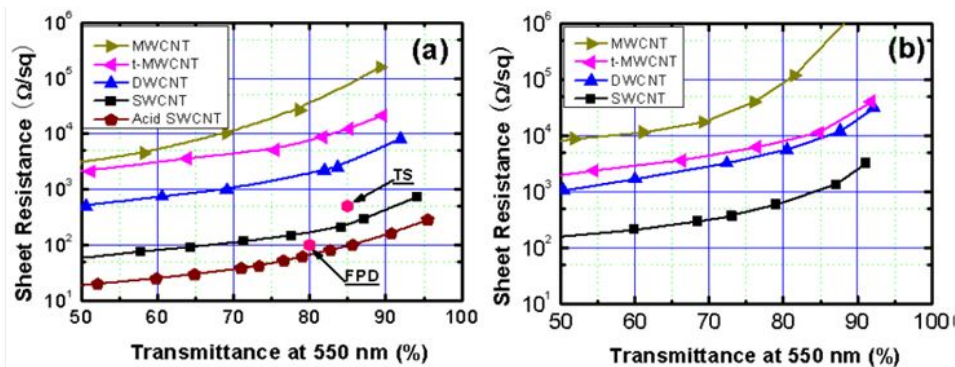


**Figure 4.** Characteristic sheet resistance-transmittance curves for various CNT-films. Each curve contains several data points from films with different numbers of sprays by a CNT solution dispersed in (a) deionized water with SDS and (b) DCE without dispersant. Reprinted with permission from reference [9].

SWCNTs synthesized by different methods such as arc discharge (Arc), catalytic chemical vapor deposition (CVD), high pressure carbon monoxide (Hipco), and laser ablation (Laser) were also analyzed systematically [20]. After the SWCNT powder was characterized, each of them was dispersed in deionized water with sodiumdodecyl sulfate (SDS) by sonication followed by aspray process to fabricate the SWCNT film onto PET substrates. By analyzing the SWCNT film performance varying with the SWCNT parameters, they found that the metallicity of the SWCNTs extracted from G'-band intensity of Raman spectroscopy and the degree of dispersion in the solution are the most decisive factors in determining the film performance. Figure 5 shows that the film performance changes dramatically with different types of SWCNTs. The TCFs fabricated with Arc SWCNTs result in the best film performance, consistent with previous report [22]. The sheet resistance of the Arc TCF is  $\sim 160 \Omega/\text{sq}$  at a transmittance of 80%, which can be used in a wide range of applications from touch panels to electrodes for future flexible displays.

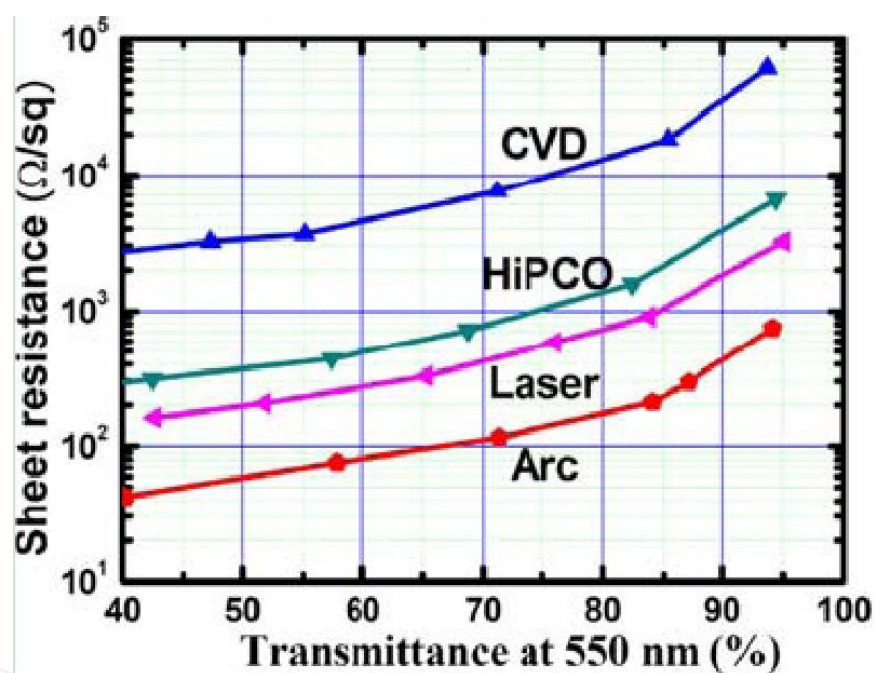


**Figure 5.** Characteristic curves of sheet resistance-transmittance of TCFs fabricated by various SWCNTs. Reprinted with permission from Ref. [20].

In order to investigate the underlying reason, CNTs were characterized with SEM, TEM, TGA and Raman spectra. TEM analysis showed that the diameter of individual nanotube synthesized with CVD and Hipco process were about 1nm, smaller than those ( $\sim 1.4$  nm) of Laser and Arc SWCNTs. The CVD SWCNTs had the smallest average bundle size, as estimated from the SEM images, whereas the Laser sample exhibited the largest average bundle size among samples. Carbonaceous particles on the SWCNT bundles are present in the CVD SWCNTs. The Arc SWCNTs have relatively well-defined crystallinity without amorphous carbon on the tube walls, although the bundle size of the Arc sample is smaller than that of the Laser sample. Figure 6 disclosed that the influence of the purity of the SWCNT is



less deterministic, particularly in CVD and HiPCOSWCNTs, where as the diameter has a strong correlation to the sheet conductance of SWCNT film. The sheet conductance of the film increases consistently with increasing diameters of nanotubes, as shown in Figure 6. This can be attributed to the decreasing band gap with increasing diameters of semi-conducting SWCNTs. Although individual metallic tubes are independent of the diameters, there are usually a pseudogap induced by tube-tube interactions, which is also inversely proportional to the tube diameter. Thus, the conductivity of the metallic nanotubes reveals the similar diameter dependence to semiconducting ones.

The radial breathing modes (RBM) of Raman spectra were used to characterize the metallicity of SWCNTs [20]. At 514 nm, the Laser and Arc SWCNTs reveal the semiconducting behavior exclusively, on the other hand, CVD and HiPCOSWCNTs contain both metallic and semiconducting nanotubes. At 633 nm, the Laser and Arc SWCNTs pick up mostly metallic SWCNTs, where as the CVD SWCNTs retain mostly semiconducting properties (less prominent Fano line) and the HiPCOSWCNTs contain both the metallic and the semiconducting behaviors. Other than RBM mode, the  $G'$ -band intensity is strongly correlated with the metallicity of SWCNTs. Despite the abundance of metallicity, the presence of defects on the nanotube walls that may act as scattering centers degrades the conductivity of the SWCNT network [23]. The intensity of the D-band indicates the amount of defects on the nanotube walls. Therefore, an appropriate parameter to express conductivity of nanotubes for SWCNTs is the intensity ratio,  $G'$ -band/D-band. High content of metallicity and few defects on the nanotube walls will be desired for high conductivity of the SWCNT films.

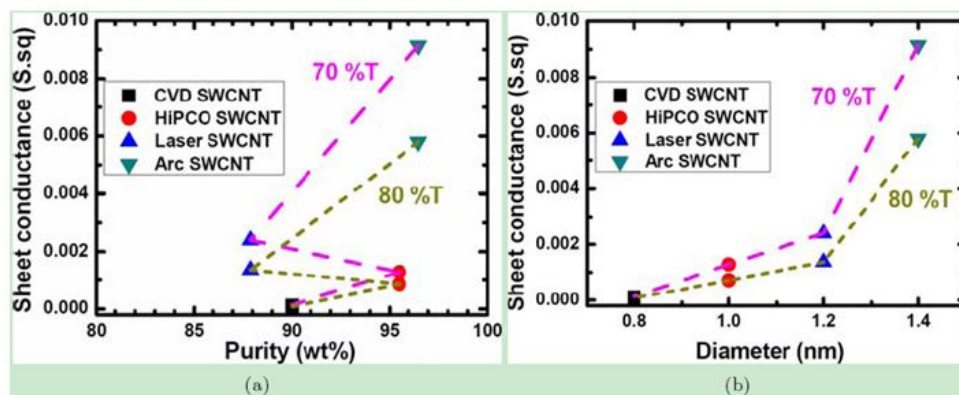


**Figure 6.** The sheet conductance of TCFs at transmittance of 70% and 80% versus (a) purity and (b) diameter of SWCNT powders. Reprinted with permission from Ref. [20].

The purity affects the conductivity. The diameter contributes to the conductivity via bandgap described in the previous paragraph. More defects reduce the *mean free path* of carriers and decrease the mobility of carriers in nanotubes. The conductivity is proportional to the metallicity of nanotubes and inversely proportional to the number of scattering centers or defects [24-26]. Considering all these factors, a material quality factor  $Q_m$  was defined to govern the conductivity of SWCNTs:

$$Q_m = P \times \left( e^{E_{pg}/2k_B T} \times \overline{\sum I_M} \right) + e^{-E_q/2k_B T} \times e^{(E_i - E_f)/k_B T} \times \overline{\sum I_S} \quad (6)$$

where  $E_g = 0.82/D$  (eV),  $E_{pg} = 0.105/D$  (eV),  $D$  is the average diameter of individual SWCNTs,  $P$  is the purity of the sample,  $E_i$  is the intrinsic Fermi Level,  $E_f$  is the Fermi Level for the extrinsic semiconductors,  $k_B$  is the Boltzmann constant and  $T$  is the temperature of the system. Here  $I_S$  ( $I_M$ ) is defined as

$$I_S(I_M) = I_{G'D} \times \frac{A_S(A_M)}{A_M + A_S} \quad (7)$$

where  $A_S(A_M)$  is the areal intensity of semiconducting (metallic) peaks of RBMs from Raman shift. After calculation, it was observed that the sheet conductance reveals a linear relationship with the material quality factor. Although this empirical formula is not rigorous, it can provide at least a means to estimate material quality that governs the conductivity of the SWCNTTCFs. For instance, large diameter, higher purity, less defects (lower intensity of D-band), and more metallic nanotubes (higher intensity of G'-band) will give better conductivity of the SWCNTTC. From this point of view, the Arc TCF is the best sample providing the highest conductivity in comparison to TCFs made by other types of SWCNTs.

In addition to the material parameters discussed above, the length of SWCNTs is also crucial to the TCF performance. According to the percolation theory, a conducting path could be formed at a lower density for longer nanotubes, which means at the same sheet resistance, TCFs prepared with longer nanotubes should exhibit higher optical transparency. This conjecture has been confirmed by experiments [27,28]. In order to optimize the CNTs quality, such as their purity, their dispersibility and the content of metallic tubes, some pretreatments need to be done. Several attempts have been tried to purify the CNT powders. Generally, Gas phase reaction or thermal annealing in air or oxygen atmosphere is used to remove amorphous carbon [29,30]. The key idea with these approaches is a selective oxidative etching processes, based on the fact that the etching rate of amorphous carbons is faster than that of CNTs. Since the edge of the CNTs can be etched away as well as carbonaceous particles during the annealing, it is crucial to have a keen control of annealing temperatures and annealing times to obtain high yield. Liquid-phase reactions in various acids are always conducted to remove the transition metal catalysts [31-33]. Hydrochloric acid, nitric acid and sulfuric acid are the most commonly used acid, and the purification effect is dependent on the concentration, the reaction temperature and the reaction time. In addition to their reaction with metal catalysts, nitric acid and sulfuric acid could induce some carboxyl or hydroxyl groups onto the walls of nanotubes, which will improve their dispersibility in water [34,35]. However, some damages were introduced during this process. Therefore, subsequent annealing or ammonium treatment was sometimes carried out to repair the wall structures of the nanotubes to fulfill some special requests.[36]. In order to enhance the con-

tent of metallic tubes, discriminated adsorption and separation or ion change chromatography was generally used.

#### 4. CNT Ink Preparation

One of the major advantages in using CNTs over more conventional metal oxides is their ability to be applied to substrates from solution, which opens up many alternative deposition techniques. Therefore, one of the primary areas of research for making transparent conductive films is finding ways to process the CNT materials into printable inks. The first part of the ink making process is in finding suitable ways to disperse the CNT material into solution. Commercial SWCNTs always aggregated into thick bundles due to their high surface energy and strong van der Waals force between tubes. However, the conductivity of the SWCNT TCFs is inversely proportional to the bundle size considering tube-tube junction resistance [37]. Therefore, it is crucial to exfoliate SWCNT thick bundles into thinner or even individual ones.

There are three major approaches to dispersing CNTs:

- a. dispersing CNTs in neat organic solvents [38,39];
- b. dispersing CNTs in aqueous media with the assistance of dispersing agents such as surfactants and biomolecules [40];
- c. introducing functional groups which will help draw the CNTs into solution [41].

Each of these methods has advantages and disadvantages in terms of making processable CNT based inks.

Direct solubilization of CNTs in a suitable solvent is perhaps the simplest and the most favorable method from a manufacturing point of view, since there are no solubilization agents involved which could create processing issues during manufacturing, and also lead to decreased conductivity in the as deposited film. A range of solvents have been tried to exfoliate SWCNTs, and exhibit tremendous differences on the efficiency. The major issue with using these organic solvents has been the inability to disperse CNTs at a concentration high enough to be useful for industrial applications ( $>0.1$  g/L). Recently, work by Prof. Coleman's group [42] has shown that the solvent cyclohexylpyrrolidone (CHP) can disperse CNTs up to 3.5 g/L with high levels of individual tubes or small bundles and can keep stable for at least one month. However, the high boiling point of this solvent may be an issue in high speed roll-to-roll manufacturing on plastic. Continuing to search for optimal solvents which can disperse CNTs at high concentrations and have a reasonably low boiling point (150 °C or below) could lead to a facile manufacturing process for high performance transparent conductive films.

Over the years, significant efforts have been devoted to finding a suitable parameter to guide the selection of good solvents. Three major theories have been proposed, which are

non-hydrogen Lewis base theory, [43] polar  $\pi$  system and optimal geometry theory [44] and Hansen parameter [42]. According to non-hydrogen Lewis base theory, all of the solvents can be divided into three groups on the basis of their properties. Class 1 consists of the best solvents, *N*-methylpyrrolidone (NMP), *N,N*-dimethylformamide (DMF), hexamethylphosphoramide (HMPA), cyclopentanone, tetramethylenesulfoxide and  $\epsilon$ -caprolactone (listed in decreasing order of optical density of the dispersions), which readily disperse SWNTs, forming light-grey, slightly scattering liquid phases. All of these solvents are characterized by high values for electron-pair donicity  $\beta$  [45], negligible values for H-bond donation parameter  $\alpha$ , [46] and high values for solvchromic parameter  $\pi^*$ . Thus, *Lewis basicity* (availability of a free electron pair) without H-donors is key to good solvation of SWNTs. Class 2 contains the good solvents, toluene, 1,2-dimethylbenzene (DMB),  $\text{CS}_2$ , 1-methylnaphthalene, iodobenzene,  $\text{CHCl}_3$ , bromobenzene and 1,2-DCB. They show  $\alpha \approx \beta \approx 0$  and high value of  $\pi^*$ . Class 3 entails the bad solvents, *n*-hexane, ethylisothiocyanate, acrylonitrile, dimethyl sulfoxide (DMSO), water and 4-chloroanisole. Bad solvents would have  $\alpha = \beta = \pi^* \approx 0$ . However, the high electron-pair donicity alone has proven to be insufficient, as dimethyl sulfoxide (DMSO) is not an effective solvent for SWNTs even though it contains three lone pairs [47]. A systematic study of the efficiency of a series of amide solvents to disperse as-produced and purified laser-generated SWNTs suggested that the favorable interaction between SWNTs and alkyl amide solvents is attributable to the highly polar  $\pi$  system and optimal geometries (appropriate bond lengths and bond angles) of the solvent structures [48]. However, this conclusion is somewhat undermined by the poor solubility of SWNTs in toluene [47]. Recently, Coleman et al found that the dispersibility of SWCNTs was intimately related with the Hansen parameters of the solvents and it is more sensitive to the dispersive Hansen parameter than the polar or H-bonding Hansen parameter. The dispersion, polar, and hydrogen bonding Hansen parameter for the nanotubes is estimated to be  $\langle \delta_D \rangle = 17.8 \text{ MPa}^{1/2}$ ,  $\langle \delta_P \rangle = 7.5 \text{ MPa}^{1/2}$ , and  $\langle \delta_H \rangle = 7.6 \text{ MPa}^{1/2}$ . Successful solvents exist in only a small volume of Hansen space, which is  $17 < \delta_D < 19 \text{ MPa}^{1/2}$ ,  $5 < \delta_P < 14 \text{ MPa}^{1/2}$ ,  $3 < \delta_H < 11 \text{ MPa}^{1/2}$ . Hansen parameters have been used successfully to aid solvent discovery. Unfortunately they are not perfect. A number of non-solvents exist in the region of Hansen parameter space close to the solubility parameters of nanotubes.

Compared with organic solvent, it is more efficient to exfoliate SWCNTs into thin bundles or even individual tubes with the assistance of dispersants. The most common dispersants used in TCFs are anionic surfactants including sodium dodecyl sulphate (SDS) and sodium dodecylbenzenesulphonate (SDBS). They are preferable dispersants because nanotubes can be highly exfoliated by them at rather high concentrations [49]. Besides, they nearly have no absorption over the visible spectrum region. However, they are not without disadvantage. Large amount of them is needed to exfoliate nanotubes into thin bundles; usually the CMC (critical micelle concentration) value should be reached [50]. Their residue will increase the sheet resistance of nanotube films significantly since they are nonconductive. In recent years, a lot of research has been done on the dispersion of CNTs with biomolecules such as DNA and RNA [51-54]. There are a number of advantages using them as dispersants. First, they can coat, separate, and solubilize CNTs more effectively with their phosphate backbones interacting with water and many bases binding to CNTs [55]. DNA wrapped around

CNTs helically and there were strong  $\pi$ - $\pi$  interactions between them [56]. Charges were transferred from the bases of DNA to CNTs leading to the change of their electron structures and electrical property [57]. 1 mgDNA could disperse an equal amount of as-produced HiP-COCNT in 1 ml water, yielding 0.2 to 0.4 mg/ml CNT solution after removal of non-soluble material by centrifugation. Such a CNT solution could be further concentrated by ten-fold to give a concentration as high as 4 mg/ml [52]. Jeynes's research disclosed that total cellular RNA showed better dispersion ability than dT(30) which was the most effective oligonucleotide dispersants in previous reports [54]. Second, the amount of DNA needed to exfoliate CNTs into thin bundles was much less than common surfactants such as SDS. In Zheng's work, the weight ratio between SWCNTs and DNA was 1:1 [52] while the dosage of RNA in Jeynes's work was lower, only half amount of the nanotubes [54]. By contrast, ten fold of SDS was needed to exfoliate SWCNTs efficiently [11,58]. High dosage of dispersant is not preferred since they are nonconductive and their residue will decrease the conductivity of the films significantly. Third, they have little absorption over the visible range and will not decrease the transmittance of CNT films. Last but not least, as biomolecules, they are easily degraded and removed by acid, base or appropriate enzyme. Jeynes et al [54] have used RNA to disperse CNTs and digested them by RNase effectively.

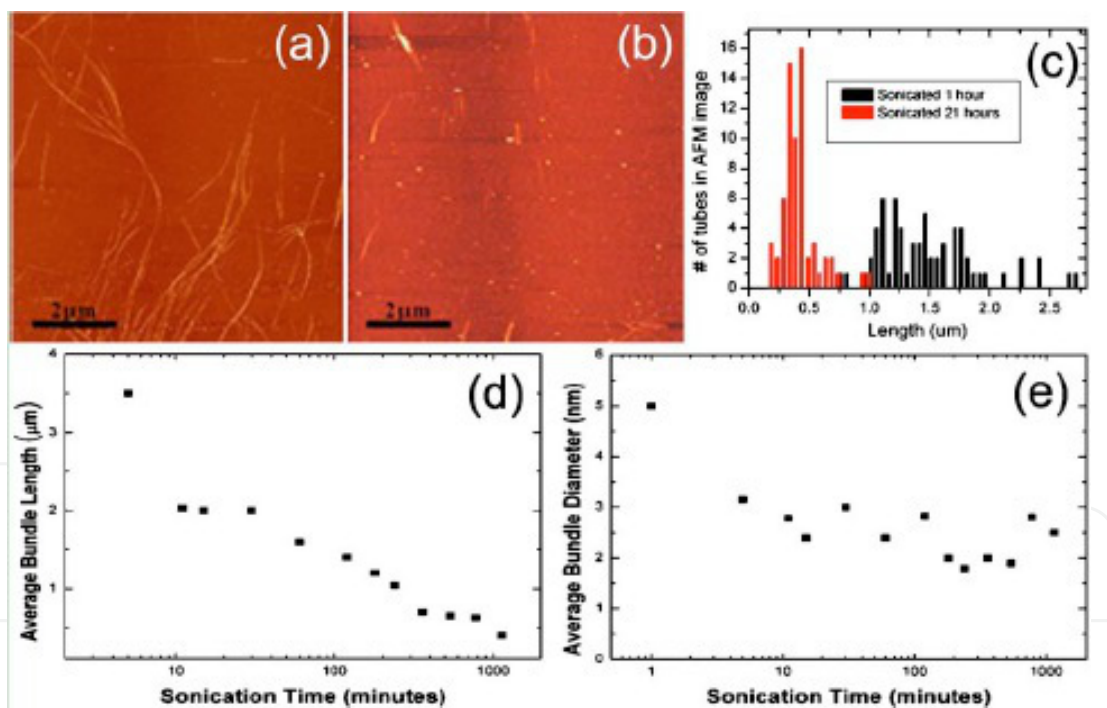


**Figure 7.** Effects of sonication on SWNT bundle length and diameter. (a) and (b) AFM image of SWNTs absorbed on a silicon wafer after (a) 1 h and (b) 21 h of sonication time. (c) Histogram of bundle length distribution taken from several AFM images for 1 h (black) and 21 h (red) of sonication. Plot of the (d) average bundle diameter and (e) average bundle length for various sonication times measured from AFM images. Reprinted from Ref. [37] copyright AIP.

The final solubilization approach involves functionalizing CNT walls with covalently bonded molecules. The most commonly used process is introducing carboxyl groups by reacting with concentrated acid, such as nitric acid and sulfuric acid [59]. Although this method has

been proven to lead to CNT solutions with high concentrations of thin bundles, the films made from these tubes tend to have extremely low conductivity values, as the functionalization procedure induces defects into the pristine CNTsp<sup>2</sup> bond structure.

For all solubilization approaches, energy must be imparted to the system to break the strong van der Waals force between tubes. This is commonly done by mixing techniques such as high-shear mixing, rotor-stator, three-roll milling, ball milling, homogenizers, and ultrasonication. Among these, ultrasonication is the most commonly used and the most efficient technique to prepare SWCNT water solution. The vibration of the sonication tip in the solution causes pressure waves which expand and collapse dissolved gas in the liquid; the collapse of these bubbles causes temperature of local zones exceeding 10 000 °C, [60] which can impart enough energy to separate CNTs from each other, long enough for surfactants to surround the tubes and prevent them from aggregating. However, such high energy of sonication would introduce defects onto the walls of CNTs or even shorten them [37]. As seen from Figure 7, the diameter of the bundles decreases sharply from 5 to 3 nm in the first 5 min of sonication, and then remains 2-3 nm after that. However, the length of the tubes decreases exponentially with sonication time from 4 μm initially, to 0.4 μm after about 21 h of sonication. Therefore, suitable sonication powder and time needs to be chosen to make SWCNT inks with thin bundles and long length.

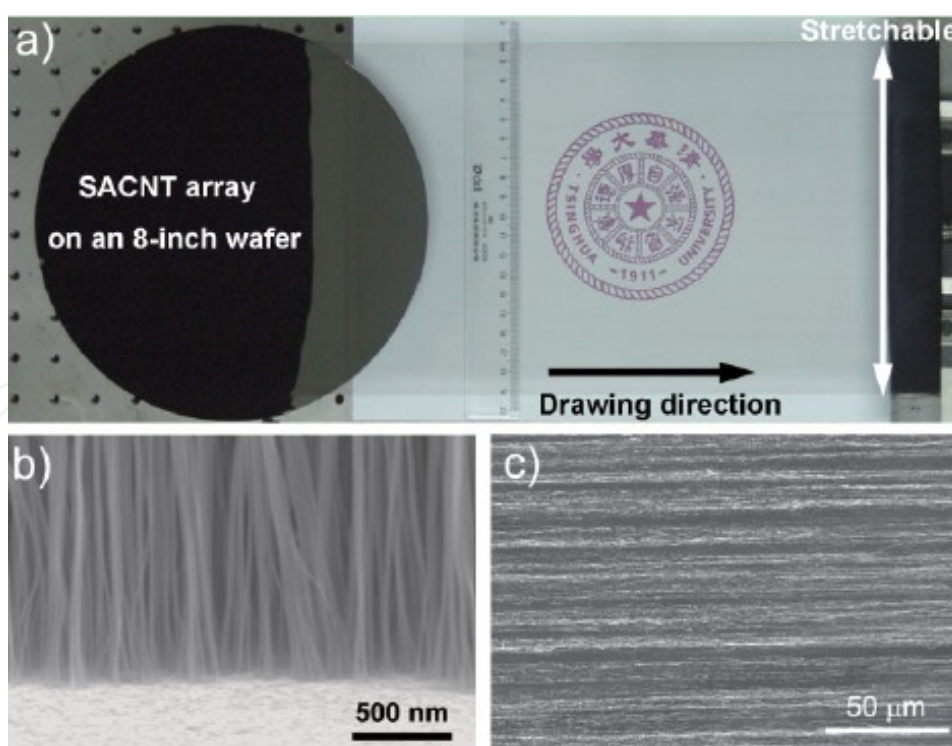


**Figure 8.** Freestanding SACNT film drawn out from a 230-mm-high SACNT array on an 8-inch silicon wafer. The film in the visual field is about 18 cm wide and 30 cm long. b) SEM image of the SACNT array on the silicon wafer in side view. c) SEM image of an SACNT film in top view. Reprinted with permission from Ref. [63] copyright Wiley

## 5. Film Fabrication

Many techniques have been developed to prepare CNT thin films, including both dry and solution-based methods. Although solution-based techniques are the mostly commonly used and industry preferred, dry method is negligible for preparing high performance TCFs. Direct growth of CNT films is one of the typical dry method. CVD can grow CNT films either randomly distributed or aligned by controlling the gas flow, catalyst patterns, or by using a substrate with a defined lattice structure [61]. Compared with a solution-based process, the direct growth method leads to films with individually separated tubes with fewer defects and better CNT-CNT contact, which leads to highly conductive films [62]. However, films directly grown on a substrate may have significant amounts of residual catalyst, imprecise density control, and substrate incompatibility for device integration. Furthermore, CVD is a high vacuum, high temperature process and is not compatible with substrates used in the emerging plastic electronics field.

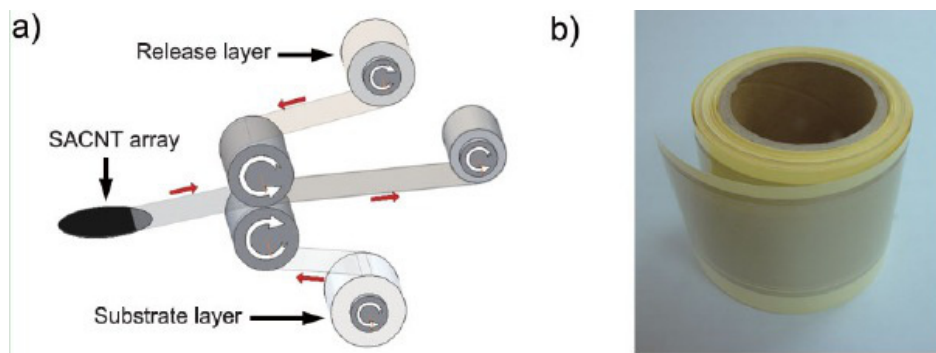


**Figure 9.** Production and performance of SACNTTCFs. a) Illustration of the roll-to-roll setup for producing composite TCFs. b) A reel of SACNT/PE composite TCF produced by the roll-to-roll setup. The grey central region of the reel is the SACNT/PE composite TCF. Reprinted with permission from Ref. [63] copyright Wiley.

In 2002, a method was pioneered by Dr Fan's group [63] and involves drawing out MWCNT films directly from as-grown super aligned CNT (SACNT) arrays. An example of such process and films are shown in Figure 8. An SACNT array is a special kind of vertically aligned MWCNT array having a higher surface density and better alignment of MWCNTs than an ordinary one. Typically, an SACNT array with an area of  $0.01 \text{ m}^2$  can be totally converted to a SACNT film of  $\sim 6\text{--}10 \text{ m}^2$ , depending on the height of the SACNT array. Unlike the solution-based process, an entire SACNT array can be converted to films without any significant loss by the drawing process, which will lower the cost. Another crucial advantage of this solution-free process is that it can be straightforwardly incorporated into a roll-to-roll process to make SACNT/polymer-sheet composite films. In a roll-to-roll process as shown in Figure 9a, a SACNT film is drawn out, then sandwiched by a release layer and a substrate layer, and pressed by two close rollers tightly, forming an SACNT/substrate composite film. The release layer, such as a slick paper, protects the SACNT film from sticking to the roller, and can be peeled off when using the film. Figure 9b shows a reel of SACNT/polyethylene (PE) composite film that is produced from an entire wafer of SACNT array. The width of the film

in this reel is about 8 cm, and the length can be over 60 m. In principle, by periodically inserting a new SACNT source wafer, the composite film can be produced continuously by the roll-to-roll process. Unfortunately, the performance of such as-drawn films is far below our expectation. In order to improve their performance, the SACNT arrays were trimmed by the oxygen plasma to reduce their height, since lower arrays give rise to films without large bundles. Besides, the SACNT films were trimmed by lasers to burn the outmost CNTs of the bundles and to make the bundles thinner. After treatment, films with excellent performance ( $24 \Omega/\text{sq}$  @ 83.4%,  $208 \Omega/\text{sq}$  @ 90%) were obtained, and successfully used as touch panels.

Compared with dry method, solution-based method is much easier to prepare CNT films with high reproducibility. Perhaps the simplest way to make CNT films is by filtering the solution of dispersed tubes over a porous filter membrane. Filtration leads to highly uniform and reproducible films, and has precisely control over density [64]. Therefore, this method is often used to evaluate CNT materials and dispersion quality. Deposition method does not have the issues on the wetting on various substrates and it works well with extremely dilute CNT solutions. Another merit deserve to be addressed is that some excess dispersants could be washed away during the filtering process, which could enhance the conductance of the films. To our experience, films prepared with filtration method always show higher conductance than films prepared with spray coating or rod-coating method, since all of the dispersants resided in the films in the later methods. Since the films are deposited onto filters, a transfer from filters to other substrates is generally needed. Accordingly, transfer methods such as PDMS method [65]. Laser transfer method and microwave assisted method were developed [66]. The limitation of this method is that the size of the films is constrained by the filter, and is difficult to scale up. It is likely that this method will continue to be restricted to academic research.

In addition to vacuum assisted filtration, there are other deposition techniques that are useful for small scale lab testing. These include spray coating, [11] spin coating, [67] dipcoating, [68] and draw-downs using a Mayer rod or Slot Die [69]. Spray coating is a simple and quick method to deposit CNT films. Typically, CNT ink is sprayed onto a heated substrate. The substrate is heated to facilitate the drying of the liquid. The set temperature for the substrate is adjusted by the choice of solvent. By using diluted solution and multiple spray coating steps, homogeneous films can be obtained. Bundling may happen during the drying process after the sprayed mist of CNT has hit the PET substrate. Thus, it is difficult to get good film uniformity. The most widespread deposition method involves depositing solution on a substrate by Mayer Rod or Slot Die, followed by controlled drying. A heating bar is used to control the drying process. This technique can be used to coat directly onto polyethylene terephthalate (PET), glass, and other substrates at room temperature and in a scalable way. Inkjet printing is an old and popular technology due to its ability to print fine and easily controllable patterns, noncontact injection, solution saving, and high repeatability [62]. It is very prevalent in printed electronics. In a typical ink jet printing process, the droplet size is around  $\sim 10$  pL and, on the substrate, has a diameter of around  $20\text{--}50 \mu\text{m}$ . Printing on paper is much easier than printing on a plastic or glass substrate, due to the high liquid absorption of the paper, which avoids the dewetting of the liquid on substrates. The liquid droplet and



substrate interaction is crucial for uniform drying of the liquid. The most useful deposition technique is roll to roll coating of CNT inks onto continuous rolls of plastics. This technique can coat film up to 2 m wide at speeds up to 500 m/min. One such roll-to-roll coating line running continuously would have the equivalent output of 30 traditional sputter coaters, and could produce enough film to satisfy half of the available touch panel market. Examples of various film fabrication methods were shown in Figure 10.

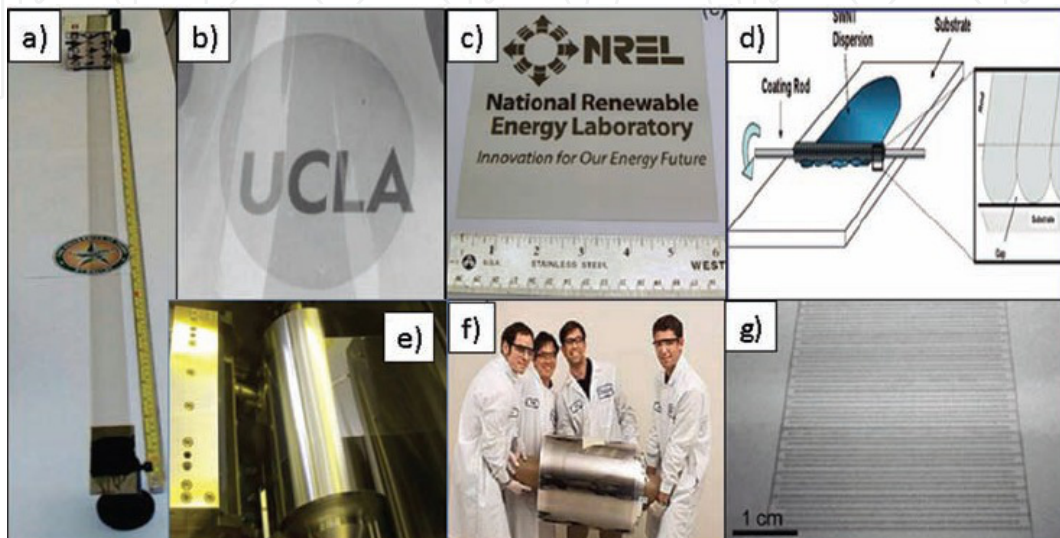


**Figure 10.** a) Transparent CNT film pulled from vertically grown CNT forest; b) CNT film transferred to PET using PDMS stamp. c) CNT film spray coated onto large area plastic; d) Mayer rodcoating schematic. e) Image of CNT film being coated by slot die f) Roll of printed CNT film. g) Inkjet printed CNT lines. Reprinted with permissions from Ref. [4] copyright Wiley

## 6. Post-Treatment of CNT Films

During the preparation of CNT water solutions, dispersants are always introduced to assist the exfoliation of CNT bundles. Since these dispersants are insulating, their residue decreases the conductance of CNT films significantly. Hence, post-treatments to remove these dispersants are necessary for preparing TCFs with high performance. In addition to removing the dispersants, doping is the other goal of post-treatment. In addition to rinsing with water, acid treatment is the most commonly used method to post-treat CNT films. As reported by Geng,<sup>11</sup> the sheet resistance of CNT films reduced by a factor of 2.5 times after treatment in concentrated nitric acid owing to the removal of surfactants SDS. Except for their function on removing dispersants, concentrated nitric acid is often used to p-dope CNTs and enhances their conductivity [70]. Although nitric acid was effective to remove dispersants, it induced p-doping of CNTs, which will lead to instability of the films [71]. Besides, PET substrates will turn brittle after long time acid treatment. To solve this problem, Dr Sun's group developed a novel technique combining base treatment and short time acid treatment [72]. In their work, biomolecule RNA was chosen as the dispersant since they are easily degraded by base, acid

and RNase. After depositing CNT films onto a PET substrate, they were immersed in the 5 wt % NaOH solution for one hour, and then treated with nitric acid for 10 min. The sheet resistance decreased significantly after treatment with NaOH solution owing to the removal of RNA molecules. After treatment with nitric acid, the RNA molecules were removed further and SWCNTs were slightly doped, therefore, the sheet resistance was reduced further. Base treatment combining short time acid treatment could remove RNA molecules efficiently as well as retaining the flexibility of PET substrates and the stability of the films.

## 7. Application of CNTTCFs

CNTTCFs have found a range of applications, among which we focus on the touch screens, flat panel displays, solar cells and OLEDs.

Touch screen is almost omnipresent in our daily life, such as in cell phones, tablet computers and many other electronics. Transparent electrodes are an essential component in most types of touch screens. High optical transmittance ( $> 85\%$ ) and low sheet resistance  $R_s$  ( $< 500 \Omega/\text{sq}$ ) are normally needed for touch screens. Meanwhile, extremely excellent durability, flexibility, and mechanical robustness are required given that the touch screen may be under indentation for millions of times. The mechanical robustness demonstrated by CNT touch panels give promises for increasing the lifetime and durability of current touch screens. There are a variety of touchscreen technologies that sense touch in different ways. Figure 11a shows the basic device structure and the transparent conductor arrangement for a 4-wire analog resistive touchpanel. These panels use two continuous electrodes separated by hemispheres of polymeric "spacer dots" that are 10–100  $\mu\text{m}$  in radius and 1–2.5 mm apart. Only at the edges (where electrode attachment occurs) is the transparent electrode patterned. Surface capacitive devices share the same type of continuous conductor whereas the projected capacitive device uses transparent conductors with specific patterning into predefined geometries. Resistive touch panels function by current driven measurements and capacitive devices depend on capacitive coupling with the input device. Both panel types utilize signal processing controllers to determine X-Y and sometimes Z position of inputs.

The mechanical durability of the transparent conductors is very important for resistive touch panels, since it involves compressive, shear, and tensile stress every time it works. Their working process can be summarized as [4]:

1. Deformation of the touch side electrode—compressive, tensile
2. Contact of the touch side and device side—compressive, shear
3. Contact of touch side electrode with spacer dots—compressive, shear
4. Extreme deformation of touch side electrode near edge seal—high tensile.

Compressive stress is not required to activate the projected capacitive (ProCap) touch panels (of which the iPhone is a prime example). The ProCap touch panels are activated by a capacitive coupling with a suitable input device. Thus, there will not be the mechanical flexing is-

sues in ProCap devices. Still, the mechanical properties of the conducting layer are important since the conductors may be patterned to a size as small as  $10\ \mu\text{m}$  in width. Metal oxides patterned to such small dimension become susceptible to cracking, fractures, and thermal cycling stress.

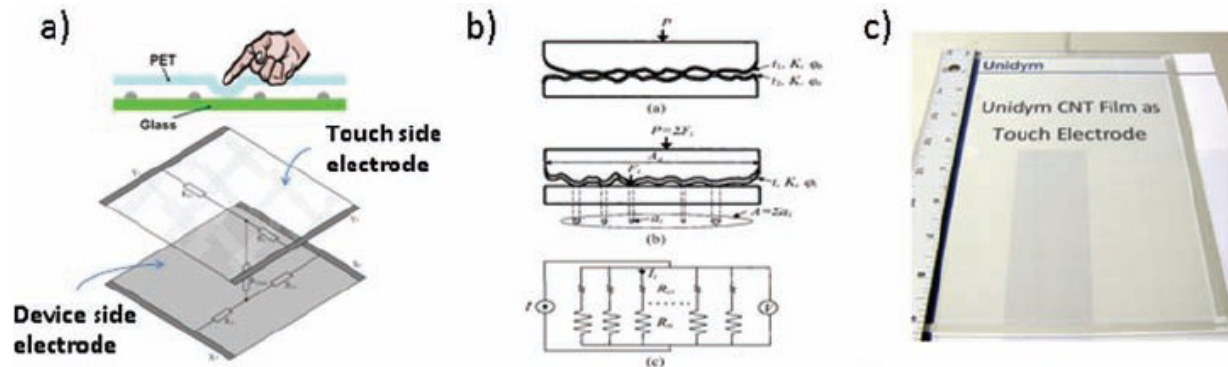


**Figure 11.** a) Schematic of four-wire resistive touch panel operation and functional layers; b) Schematic of the contact resistance experienced at the interface between two rough conductive layers separated by a very thin dielectric; c) Photograph of touch panel utilizing CNT film as touch electrode. Reprinted with permission from Ref. [4] copyright Wiley

Display panels are produced at nearly 1.7 billion units annually (1.2 billion mobile phones, 200 million televisions, 150 million laptops, and 200 million desktop, machine interfaces, monitors etc). There are four common types of displays, which are electrowetting displays (EWD), electrochromic displays (ECD), electrophoretic displays (EPD) and liquid crystal displays (LCD). Currently, LCD devices are manufactured in the greatest number and will be the main subject of this section. A transparent conductor's major role in LCD/EPD devices is to serve as pixel and common electrodes. An interesting advantage of using CNT films for LCD is the ability to use them possibly as both the transparent electrode and the alignment layer [73]. Recently, Lee et al demonstrated high performance TN-LC cells with ultra-thin and solution-processible SWNT/PS-*b*-PPP nanocomposite alignment layers. At an optimized SWNT density, a nanocomposite gave rise to low power operation with a super-fast LC response time of 3.8 ms, which is more than four times faster than that on a commercial polyimide layer due to the locally enhanced electric field around individually networked SWNTs. Furthermore, TN-LC cells with their SWNT nanocomposite layers exhibited high thermal stability up to 200 °C without capacitance hysteresis.

Transparent electrodes are the essential components for photovoltaic devices. The traditional electrodes for photovoltaic devices is ITO, which has high transmittance and low sheet resistance ( $\sim 10\text{--}20\ \Omega/\text{sq}$  with the transmittance of 90%). However, their application was constrained by the high price of indium. Besides, the brittleness of ITO limited their usage in flexible devices, which will be a developing trend in the future. Therefore, replacing materials need to be developed. Carbon nanotubes are promising candidates since they have extremely high conductivity, high work function of 4.7–5.2 eV, relatively low cost and excellent flexibility. Besides, they are easy to be deposited into film via solution based process. Glatkowski et al. [74] reported on the application of transparent CNT electrodes and found a PE-

DOT:PSS coating dramatically improves the device efficiency from 0.47% to 1.5%. The thin layer of PEDOT:PSS can smooth the CNT surface and enhance the charge transfer according to their investigation. In Hu's work, [75] flexible transparent electrodes were fabricated by printing SWCNT solutions on plastic substrates. The SWCNT films have a sheet resistance of 200  $\Omega$ /sq with a transmittance of 85%. The achieved efficiency of 2.5% (AM1.5G) approaches that of the control device made with ITO/glass (3%). Furthermore, the flexibility is far superior to devices using ITO coated on the same flexible substrate material. However, there are several aspects that need to be solved for CNT based electrodes.

1. Long term electrical stability;
2. Occasional shorting between the cathode and anode due to protruding CNTs;
3. Relatively high sheet resistance.

Light emitting diodes have an opposite light electricity coupling process as solar cells. Applications of nanoscale materials based transparent electrodes are mainly focused on organic light emitting diodes which hold great promise for the future electronics. In Aguirre's work, carbon nanotube anodes were implemented in small molecule OLED devices and achieved performance comparable to ITO-based anodes [76]. Recently, Feng et al [77] proposed a single walled carbon nanotubes-based anodes for organic light-emitting diodes (OLEDs) by spray-coating process without any use of surfactant or acid treatment. A layer of DMSO doped PEDOT:PSS was spray-coated on the SWCNT sheets to not only lessen the surface roughness to an acceptable level, but also improve the conductivity by more than three orders of magnitude. For the produced SWCNT-based OLEDs, a maximum luminance 4224  $\text{cd/m}^2$  and current efficiency 3.12  $\text{cd/A}$  were achieved, which is close to the efficiency of ITO-based OLEDs.

## Author details

Jing Sun\* and Ranran Wang

\*Address all correspondence to: Jingsun@mail.sic.ac.cn

State Key Lab of High Performance Ceramics and Superfine Microstructure, Shanghai Institute of Ceramics, Chinese Academy of Sciences, China

## References

- [1] Niu, C. M. (2011). *MRS Bull.*, 36, 766.
- [2] Tyler, T. P., Brock, R. E., Karmel, H. J., Marks, T. J., & Hersam, M. C. (2011). *Adv. Energy Mater.*, 1, 785.

- [3] Kauffman, D. R., Sorescu, D. C., Schofield, D. P., Allen, B. L., Jordan, K. D., & Star, A. (2010). *Nano Lett.*, 10, 958.
- [4] Hecht, D. S., Hu, L. B., & Irvin, G. (2011). *Adv. Mater.*, 23, 1482.
- [5] De , S., & Coleman, J. N. (2011). *MRS Bull*, 36, 774.
- [6] Tolcin, A. (2009). *Minerals Yearbook*, 35.
- [7] Green, M. A. (2009). *Progress in Photovoltaics : Research and Applications*, 17, 347.
- [8] Hu, L., Hecht, D. S., & Gruner, G. (2004). *Nano Lett.*, 4, 2513.
- [9] Geng, H. Z., Lee, D. S., Kim, K. K., Kim, S. J., Bae, J. J., & Lee, Y. H. (2008). *Journal of the Korean Physical Society*, 53, 979.
- [10] De , S., Lyons, P. E., Sorel, S., Doherty, E. M., King, P. J., Blau, W. J., Nirmalraj, P. N., Boland, J. J., Scardaci, V., Joimel, J., & Coleman, J. N. (2009). *Acs Nano*, 3, 714.
- [11] Geng, H. Z., Kim, K. K., So, K. P., Lee, Y. S., Chang, Y., & Lee, Y. H. (2007 ). *J. Am. Chem. Soc.*, 129, 7758.
- [12] Scardaci, V., Coull, R., & Coleman, J. N. (2010). *Appl. Phys. Lett.*, 97.
- [13] De , S., King, P. J., Lyons, P. E., Khan, U., & Coleman, J. N. (2010). *Acs Nano*, 4, 7064.
- [14] Jackson, R., Domercq, B., Jain, R., Kippelen, B., & Graham, S. (2008). *Adv. Funct. Mater.*, 18, 2548.
- [15] Zheng, Q. B., Gudarzi, M. M., Wang, S. J., Geng, Y., Li, Z. G., & Kim, J. K. (2011). *Carbon*, 49, 2905.
- [16] Kim, K. K., Reina, A., Shi, Y. M., Park, H., Li, L. J., Lee, Y. H., & Kong, J. (2011). *Nanotechnology*, 21.
- [17] Tantang, H, Ong, J. Y., Loh, C. L, Dong, X. C, Chen, P, Chen, Y, Hu, X, Tan, L P, & Li, L. J. (2009). *Carbon*, 47, 1867.
- [18] Saran, N., Parikh, K., Suh, D. S., Munoz, E., Kolla, H., & Manohar, S. K. (2004). *J. Am. Chem. Soc.*, 126, 4462.
- [19] Ko, W. Y, Su, J. W, Guo, C. H, & Lin, K. J. (2012). *Carbon*, 50, 2244.
- [20] Geng, H. Z., Kim, K. K., Lee, K., Kim, G. Y., Choi, H. K., Lee, D. S., An, K. H., Lee, Y. H., Chang, Y., Lee, Y. S., Kim, B., & Lee, Y. J. (2007). *Nano*, 2, 157.
- [21] Li, Z. R., Kandel, H. R., Dervishi, E., Saini, V., Biris, A. S., Biris, A. R., & Lupu, D. (2007). *Appl. Phys. Lett.*, 91.
- [22] Zhang, D. H., Ryu, K, Liu, X. L, Polikarpov, E, Ly, J, Tompson, M. E, & Zhou, C. W. (2006). *Nano Lett.* , 6, 1880.
- [23] Lyons, P. E., De , S., Blighe, F., Nicolosi, V., Pereira, L. F. C., Ferreira, M. S., & Coleman, J. N. (2008 ). *J Phys.*, 104.

- [24] Maeda, Y., Hashimoto, M., Kaneko, S., Kanda, M., Hasegawa, T., Tsuchiya, T., Akasaka, T., Naitoh, Y., Shimizu, T., Tokumoto, H., & Nagase, S. (2008). *J. Mater. Chem.*, 18, 4189.
- [25] Wang, W., Fernando, K. A. S., Lin, Y., Mezziani, M. J., Veca, L. M., Cao, L., Zhang, P., Kimani, M. M., & Sun, Y. P. J. (2008). *Am. Chem. Soc.*, 130, 1415.
- [26] Jackson, R. K., Munro, A., Nebesny, K., Armstrong, N., & Graham, S. (2010). *ACS Nano*, 4, 1377.
- [27] Sorel, S., Lyons, P. E., De , S., Dickerson, J. C., & Coleman, J. N. (2012). *Nanotechnology*, 23.
- [28] Park, J. G, Cheng, Q. F, Lu, J, Bao, J. W, Li, S, Tian, Y, Liang, Z. Y, Zhang, C, & Wang, B. (2012). *Carbon*, 50, 2083.
- [29] Ebbesen, T. W., Ajayan, P. M., Hiura, H., & Tanigaki, K. (1994). *Nature*, 367, 519.
- [30] Zimmerman, J. L., Bradley, R. K., Huffman, C. B., Hauge, R. H., & Margrave, J. L. (2000). *Chem. Mater.*, 12, 1361.
- [31] Zhang, J., Gao, L., Sun, J., Liu, Y. Q., Wang, Y., Wang, J. P., Kajiura, H., Li, Y. M., & Noda, K. (2008). *J. Phys. Chem. C*, 112, 16370.
- [32] Liu, Y. Q, Gao, L, Sun, J, Zheng, S, Jiang, L. Q, Wang, Y, Kajiura, H, Li, Y. M, & Noda, K. (2007). *Carbon*, 45, 1972.
- [33] Wang, Y., Gao, L., Sun, J., Liu, Y. Q., Zheng, S., Kajiura, H., Li, Y. M., & Noda, K. (2006). *Chem. Phys. Lett*, 432, 205.
- [34] Wang, R. R., Sun, J., Gao, L. A., & Zhang, J. (2010). *J. Mater. Chem.*, 20, 6903.
- [35] Moon, J. M., An, K. H., Lee, Y. H., Park, Y. S., Bae, D. J., & Park, G. S. (2001). *J. Phys. Chem. B*, 105, 5677.
- [36] Datsyuk, V., Kalyva, M., Papagelis, K., Parthenios, J., Tasis, D., Siokou, A., Kallitsis, I., & Galiotis, C. (2008). *Carbon*, 46, 833.
- [37] Hecht, D., Hu, L. B., & Gruner, G. (2006). *Appl. Phys. Lett.*, 89.
- [38] Bahr, J. L., Mickelson, E. T., Bronikowski, M. J., Smalley, R. E., & Tour, J. M. (2001). *Chem. Commun*, 193.
- [39] Cheng, Q. H., Debnath, S., Gregan, E., & Byrne, H. J. (2010). *J. Phys. Chem. C*, 114, 8821.
- [40] Moore, V. C., Strano, M. S., Haroz, E. H., Hauge, R. H., Smalley, R. E., Schmidt, J., & Talmon, Y. (2003). *Nano Lett.*, 3, 1379.
- [41] Chen, J., Rao, A. M., Lyuksyutov, S., Itkis, M. E., Hamon, M. A., Hu, H., Cohn, R. W., Eklund, P. C., Colbert, D. T., Smalley, R. E., & Haddon, R. C. (2001). *J. Phys. Chem. B*, 105, 2525.

- [42] Bergin, S. D., Sun, Z. Y., Rickard, D., Streich, P. V., Hamilton, J. P., & Coleman, J. N. (2009). *Acs Nano*, 3, 2340.
- [43] Torrens, F. (2005). *Nanotechnology*, 16, S181.
- [44] Landi, B. J., Ruf, H. J., Evans, C. M., Cress, C. D., & Raffaele, R. P. (2005). *J. Phys. Chem. B*, 109, 9952.
- [45] Kamlet, M. J., & Taft, R. W. (1976). *J. Am. Chem. Soc.*, 98, 337.
- [46] Taft, R. W., & Kamlet, M. J. (1976). *J. Am. Chem. Soc.*, 98, 2886.
- [47] Giordani, S., Bergin, S. D., Nicolosi, V., Lebedkin, S., Kappes, M. M., Blau, W. J., & Coleman, J. N. (2006). *J. Phys. Chem. B*, 110, 15708.
- [48] Landi, B. J., Ruf, H. J., Worman, J. J., & Raffaele, R. P. (2004). *J. Phys. Chem. B*, 108, 17089.
- [49] Islam, M. F., Rojas, E., Bergey, D. M., Johnson, A. T., & Yodh, A. G. (2003). *Nano Lett.*, 3, 269.
- [50] Ishibashi, A., & Nakashima, N. (2006). *Chem.-Eur. J.*, 12, 7595.
- [51] Zheng, M., Jagota, A., Strano, M. S., Santos, A. P., Barone, P., Chou, S. G., Diner, B. A., Dresselhaus, M. S., McLean, R. S., Onoa, G. B., Samsonidze, G. G., Semke, E. D., Usrey, M., & Walls, D. J. (2003). *Science*, 302, 1545.
- [52] Zheng, M., Jagota, A., Semke, E. D., Diner, B. A., McLean, R. S., Lustig, S. R., Richardson, R. E., & Tassi, N. G. (2003). *Nature Materials*, 2, 338.
- [53] Cathcart, H., Quinn, S., Nicolosi, V., Kelly, J. M., Blau, W. J., & Coleman, J. N. (2007). *Journal of Physical Chemistry C*, 111, 66.
- [54] Jeynes, J. C. G., Mendoza, E., Chow, D. C. S., Watts, P. C. R., McFadden, J., & Silva, S. R. P. (2006). *Adv. Mater.*, 18, 1598.
- [55] Wang, H., Lewis, J. P., & Sankey, O. F. (2004). *Phys. Rev. Lett.*, 93.
- [56] Wang, H. M., & Ceulemans, A. (2009). *Phys. Rev. B*, , 79.
- [57] Gowtham, S., Scheicher, R. H., Pandey, R., Karna, S. P., & Ahuja, R. (2008). *Nanotechnology*, , 19.
- [58] Paul, S., & Kim, D. W. (2009). *Carbon*, 47, 2436.
- [59] Marques, R. R. N., Machado, B. F., Faria, J. L., & Silva, A. M. T. (2010). *Carbon*, 48, 1515.
- [60] Hopkins, S. D., Putterman, S. J., Kappes, B. A., Suslick, K. S., & Camara, C. G. (2005). *Phys. Rev. Lett.*, 95.
- [61] Liu, P., Sun, Q., Zhu, F., Liu, K., Jiang, K., Liu, L., Li, Q., & Fan, S. (2008). *Nano Lett.*, 8, 647.

- [62] Hu, L. B., Hecht, D. S., & Gruner, G. (2010). *Chem. Rev.*, 110, 5790.
- [63] Feng, C., Liu, K., Wu, J. S., Liu, L., Cheng, J. S., Zhang, Y. Y., Sun, Y. H., Li, Q. Q., Fan, S. S., & Jiang, K. L. (2010). *Adv. Funct. Mater.*, 20, 885.
- [64] Wu, Z. C., Chen, Z. H., Du, X., Logan, J. M., Sippel, J., Nikolou, M., Kamaras, K., Reynolds, J. R., Tanner, D. B., Hebard, A. F., & Rinzler, A. G. (2004). *Science*, 305, 1273.
- [65] Cao, Q., Hur, S. H., Zhu, Z. T., Sun, Y. G., Wang, C. J., Meitl, M. A., Shim, M., & Rogers, J. A. (2006). *Adv. Mater.*, 18, 304.
- [66] Allen, A. C., Sunden, E., Cannon, A., Graham, S., & King, W. (2006). *Appl. Phys. Lett.*, 88.
- [67] Manivannan, S., Ryu, J. H., Lim, H. E., Nakamoto, M., Jang, J., & Park, K. C. (2010). *Journal of Materials Science-Materials in Electronics*, 21, 72.
- [68] Song, Y. I., Yang, C. M., Kim, D. Y., Kanoh, H., & Kaneko, K. (2008). *J. Colloid Interface Sci.*, 318, 365.
- [69] Tenent, R. C., Barnes, T. M., Bergeson, J. D., Ferguson, A. J., To, B., Gedvilas, L. M., Heben, M. J., & Blackburn, J. L. (2009). *Adv. Mater.*, 21, 3210.
- [70] Zhao, Y. L., & Li, W. Z. (2010). *Microelectron. Eng.*, 87, 576.
- [71] Graupner, R., Abraham, J., Vencelova, A., Seyller, T., Hennrich, F., Kappes, M. M., Hirsch, A., & Ley, L. (2003). *PCCP*, 5, 5472.
- [72] Wang, R. R., Sun, J., Gao, L. A., & Zhang, J. (2010). *Acs Nano*, 4, 4890.
- [73] Fu, W. Q., Liu, L., Jiang, K. L., Li, Q. Q., & Fan, S. S. (2010). *Carbon*, 48, 1876.
- [74] Van de Lagemaat, J., Barnes, T. M., Rumbles, G., Shaheen, S. E., Coutts, T. J., Weeks, C., Levitsky, I., Peltola, J., & Glatkowski, P. (2006). *Appl. Phys. Lett.*, 88.
- [75] Rowell, M. W., Topinka, M. A., Mc Gehee, M. D., Prall, H. J., Dennler, G., Sariciftci, N. S., Hu, L. B., & Gruner, G. (2006). *Appl. Phys. Lett.*, 88.
- [76] Aguirre, C. M., Auvray, S., Pigeon, S., Izquierdo, R., Desjardins, P., & Martel, R. (2006). *Appl. Phys. Lett.*, 88.
- [77] Xue, F., Zhuo, W. Q., Yanc, L., Xue, H., Xiong, L. H., & Lia, J. H. (2012). *Org. Electron.*, 13, 302.



